

FLOW APPROACH ON RIESZ TYPE NONLOCAL ENERGIES

JIAXIN HE, QINFENG LI, JUNCHENG WEI, AND HANG YANG

ABSTRACT. Via continuous deformations based on natural flow evolutions, we prove several novel monotonicity results for Riesz-type nonlocal energies on triangles and quadrilaterals. Some of these results imply new and simpler proofs for known theorems without relying on any symmetrization arguments.

1. INTRODUCTION

Let Ω be a bounded domain in \mathbb{R}^2 . Define

$$D(\Omega) = \int_{\Omega} \int_{\Omega} K(|x - y|) dx dy,$$

where $K : \mathbb{R}^+ \rightarrow \mathbb{R}$ is a C^1 , strictly decreasing function and $\int_0^1 K(r)r dr < \infty$. The last condition is to guarantee that $D(\cdot)$ is finite on bounded planar domains, as shown in [2]. $D(\Omega)$ is often called the Riesz-type potential nonlocal energies, and the prototype of $K(r)$ is given by $r^{-\alpha}$, $\alpha \in (0, 2)$.

It is a well-established fact that, in any dimension, $D(\cdot)$ is uniquely maximized by a ball under a volume constraint, thanks to Riesz's rearrangement inequality [12]. The discrete optimization problem is then natural, and it is often conjectured that, among polygons with N sides and fixed area, the regular polygon uniquely maximizes $D(\cdot)$. Surprisingly, this is in general not true, as it is proved in the very interesting work [1] that the maximality of regular polygon should be sensitive to the choice of the kernel K , when N is large.

When $N = 3, 4$, the conjecture is indeed correct, as proved earlier in [2] via an iteration of Steiner symmetrization, in the same flavor of the proof in [10, Section 7.4]. The rigidity results for triangles and quadrilaterals are also obtained in [2] along some particularly chosen shape deformations.

We are motivated by the following question:

Question 1.1. *Are there other area-preserving deformations, which are not based on the Steiner symmetrization, but along which $D(\cdot)$ is still increasing?*

This question is of significance since it can lead to new monotonicity results and provide more diverse optimization strategies. To tackle the question, we utilize the flow approach, as it not only naturally handles continuous evolution and transforms the monotonicity investigation of $D(\cdot)$ into the sign analysis of shape derivatives of $D(\cdot)$ along the flow, but also eliminates the reliance on Steiner symmetrization argument.

Research of Qinfeng Li is supported by National Key R&D Program of China (2022YFA1006900) and the National Science Fund of China General Program (No. 12471105). The research of Juncheng Wei is partially supported by GRF grant of HK RGC entitled "New frontiers in singular limits of elliptic and parabolic equations".

In this paper, we mainly focus our attention on triangles and quadrilaterals, which represent two important classes of planar domains. Though the geometries of triangles and quadrilaterals are simple, many significant results have been established on them, which often inspire further important results on generic shapes. For a comprehensive introduction on shape optimization problems on triangular domains, we refer to the classical monographs [10] and [6], as well as the excellent survey in [7, Section 6] by Laugesen and Siudeja.

Concerning Question 1.1 for triangles, the first result we obtain is the following:

Theorem 1.2. *Let $\Omega = \triangle_{ABC}$ be a triangle, with AB being the longest side and lying on the x -axis, and with C lying on the positive y -axis. Suppose that $|AB| > |BC| \geq |AC|$, and we let $C_t = (1+t)C$, $\Omega_t = \sqrt{\frac{|OC|}{|OC_t|}} \triangle_{ABC_t} = \triangle_{A_t B_t \tilde{C}_t}$, where O is the origin. Let $t_1 > 0$ be the unique number such that $|BA| = |BC_{t_1}|$. Then, for $t \in (-1, t_1)$, $D(\Omega_t) > 0$ is a strictly increasing function.*

Similarly, we also have:

Theorem 1.3. *Let O be the origin, $\Omega = \triangle_{ABC}$ be a non-obtuse triangle with AB being the shortest side and lying on the x -axis, and with C lying on the positive y -axis. Suppose that $|AB| < |BC| \leq |AC|$, and we let $C_t = (1-t)C$ and $\Omega_t = \sqrt{|OC|/|OC_t|} \triangle_{ABC_t}$. Let $t_2 > 0$ be the unique number such that $|BA| = |BC_{t_2}|$. Then, for $t \in (-\infty, t_2)$, $D(\Omega_t)$ is a strictly increasing function.*

The motivation of establishing Theorems 1.2-1.3 is as follows. A given non-equilateral triangle \triangle_{ABC} must belong to one of the following two cases:

- (1) It has exactly one shortest height.
- (2) It has at least two shortest height.

If \triangle_{ABC} belongs to the first case, then we can continuously stretch the shortest height while scaling the triangle to keep its area constant, and during the process, the triangle gradually becomes an isosceles triangle belonging to the second case. Then, Theorem 1.2 says that along the evolution, $D(\cdot)$ is really strictly increasing. If \triangle_{ABC} belongs to the second case, then it is a sub-equilateral triangle (i.e., an isosceles triangle with aperture less than or equal to $\pi/3$). Then Theorem 1.3, which is more general, gives the continuous deformation that gradually transforms such a triangle into an equilateral one by compressing the tallest height while preserving the area, thereby making $D(\cdot)$ increasing during the process.

An illustration of Theorem 1.2 and Theorem 1.3 can be seen in Figures 1.1-1.2 below, and the proof of Theorems 1.2-1.3 is by specifically constructing a time-dependent vector field η , which generates a flow map F_t mapping Ω to Ω_t , and then analyzing the sign of the derivative of $D(\Omega_t)$ via the reflection argument.

Therefore, combining the flow evolutions described in Theorem 1.2 and Theorem 1.3, we have found an area-preserving deformation path along which $D(\cdot)$ is strictly increasing, evolving any arbitrary non-equilateral triangle first into an isosceles triangle by stretching the shortest height, and then further into an equilateral one by compressing the tallest height. This answers Question 1.1 for triangles, and also gives another yet simpler proof of the fact (see [2, Theorem 1.1]) that equilateral triangles uniquely maximize the Riesz-type nonlocal energy $D(\cdot)$, without the traditional limit process of step-by-step Steiner symmetrizations.

A combination of Theorem 1.2 and Theorem 1.3 immediately implies the following new monotonicity results on isosceles triangles:

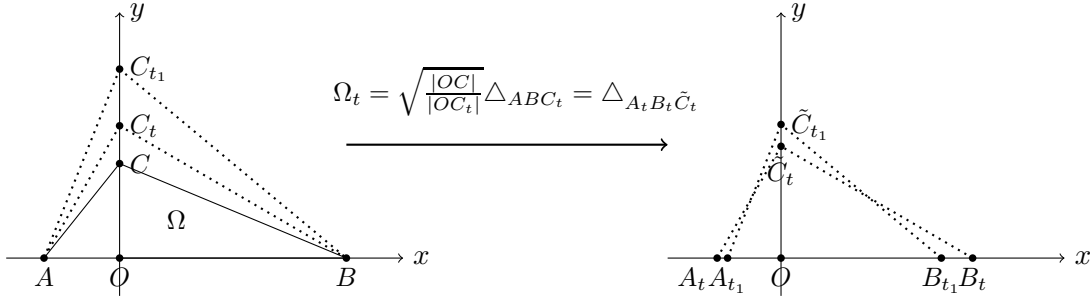


FIGURE 1.1. An illustration of Theorem 1.2 for the case when $t \in (0, t_1]$. Stretching the shortest height OC above while scaling to keep the area fixed. Then, $|\Delta_{A_t B_t \tilde{C}_t}| = |\Delta_{ABC}|$ and $D(\Delta_{A_t B_t \tilde{C}_t})$ is strictly increasing until $t = t_1$, at which time the triangle becomes isosceles.

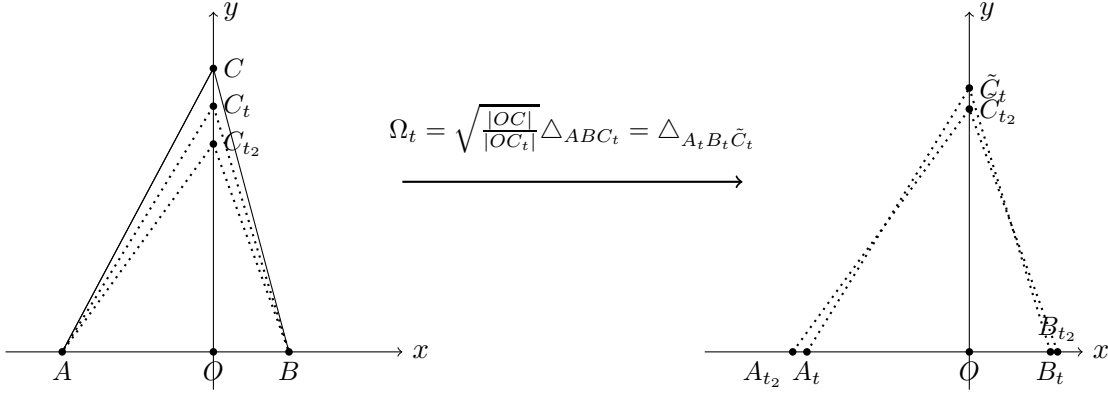


FIGURE 1.2. An illustration of Theorem 1.3 for the case when $0 < t \leq t_2$. Compressing below the tallest height OC while scaling to keep the area fixed. Then, $|\Delta_{A_t B_t \tilde{C}_t}| = |\Delta_{ABC}|$, and $D(\Delta_{A_t B_t \tilde{C}_t})$ is strictly increasing until $t = t_2$, at which time the triangle becomes isosceles.

Corollary 1.4. *Let $I(\alpha)$ be the isosceles triangle with aperture α and given area. Then, $D(I(\alpha))$ is strictly increasing when $\alpha \in (0, \pi/3)$, and is strictly decreasing when $\alpha \in (\pi/3, \pi)$.*

Similar results to Corollary 1.4 have been proved by Siudeja for Dirichlet boundary shape functionals, such as the torsional rigidity or first eigenvalue of Dirichlet Laplacian, see [11]. His argument is via both the continuous Steiner symmetrization argument and the Steiner symmetrization argument. Such monotonicity results on nonlocal energies over isosceles triangles have not been established in the previous literature.

The next result gives the strict decreasing property of $D(\cdot)$ when a triangle is strictly deviating from an isosceles one, by fixing an angle and the area while making the ratio of the longer leg to the shorter leg near that angle increasingly larger. The proof is motivated by that of Theorem 1.2. Instead of continuously stretching the height, we can continuously stretch one leg while fixing the area, which generates another flow along which $D(\cdot)$ is monotone. The transformation is illustrated in Figure 4.1.

Theorem 1.5. *Let $\Omega_{\alpha,q}$ denote the triangle of a given area, with one angle equal to α and $q \geq 1$ being the ratio of the two legs near the angle. Then, for any fixed $\alpha \in (0, \pi)$, $D(\Omega_{\alpha,q})$ is a strictly decreasing function with respect to $q \geq 1$.*

Similar type of result was also first proved by Siudeja [11] on the first eigenvalue problem of the Dirichlet Laplacian, under the additional assumption that α is the smallest angle. The proof there is by the ingenious use of polar symmetrization. Later, by delicate applications of the continuous Steiner symmetrization argument, Solynin [13] proves the strict monotonicity of the first eigenvalue without the smallest assumption on the fixed angle. The monotonicity of the Riesz-type nonlocal energy on $D(\Omega_{\alpha,q})$ has not been addressed before. Our proof via the flow method is also significantly different from previous ones used in [11] and [13]. Such ideas have also been recently applied by us to study Dirichlet shape optimization problems, see [8].

Note that Theorem 1.5 enables us to compare the magnitudes of $D(\cdot)$ on two triangles, if they have one same angle and the same area. It is then a natural question of comparing the magnitudes of $D(\cdot)$ on two triangles if they have one same side and the same area. Motivated by [3] and [2], we prove the following result, which gives another way of continuously deviating an isosceles triangle while $D(\cdot)$ is strictly decreasing during the deviation process.

Theorem 1.6. *Let $T_{l,q}$ denote the triangle of a given area, with one side equal to l and $q \geq 1$ being the ratio of the other two sides. Then, for any fixed $l > 0$, $D(T_{l,q})$ is a strictly decreasing function with respect to $q \geq 1$.*

In summary, Theorem 1.2, Theorem 1.5 and Theorem 1.6 together give three different ways of smoothly evolving an arbitrary non-isosceles triangle into an isosceles one, and during the evolutions, $D(\cdot)$ is always strictly increasing.

Next, we consider Question 1.1 on quadrilaterals. It seems to us that the monotonicity of $D(\cdot)$ under continuous Steiner symmetrization has not been stated in the previous literature. Highly motivated by [2] and [3], we prove a slightly stronger result for a class of quadrilaterals: $D(\cdot)$ is strictly increasing under a partial continuous Steiner symmetrization, see Proposition 6.2 and Figure 6.3 in section 6. For the other quadrilaterals, the monotonicity under the partial symmetrization in Proposition 6.2 is in general not true. Nevertheless, the monotonicity property of $D(\cdot)$ always holds for all quadrilaterals under the continuous Steiner symmetrization about the line perpendicular to one of the diagonals, as stated in Theorem 1.7 below.

Theorem 1.7. *Let Ω_t be the continuous family of quadrilaterals with vertices $A_t = (x_A(1-t), y_A)$, $B = (a, 0)$, $C_t = (x_C(1-t), y_C)$ and $D = (-a, 0)$, where $a > 0$, $x_A, x_C \in \mathbb{R}$ and $y_A y_C < 0$. If both x_A and x_C are not zero, then $D(\Omega_t)$ is a strictly increasing function for $0 \leq t \leq 1$.*

When the vertex $A = A_0$ changes to A_1 and the vertex $C = C_0$ changes to C_1 at time $t = 1$, the quadrilateral turns into a kite. Then, we can similarly move the vertices B and D up or down to turn the kite into a rhombus. By Theorem 1.7, $D(\cdot)$ is strictly increasing along the continuous deformation. Up until the point of deformation into the rhombus, the monotonicity of $D(\cdot)$ is essentially through the continuous Steiner symmetrization process. However, beginning with the rhombus, motivated by Theorem 1.2, we employ another transformation as follows: we continuously compress the longer diagonal of the rhombus until the two diagonals are equal, while always scaling to fix the area during the deformation.

This step does not involve any continuous symmetrization argument, and we still have the monotonicity result, as stated below.

Theorem 1.8. *Let Ω_q be the rhombus with a given area, where $q \geq 1$ is the ratio of the lengths of the diagonals of the rhombus. Then, $D(\Omega_q)$ is a strictly decreasing function for $q \geq 1$.*

As a particular application of Theorem 1.7 and Theorem 1.8, we also obtain another proof of the fact (see [2, Theorem 1.1]) that the squares uniquely maximize the Riesz-type nonlocal energy $D(\cdot)$, by finding a continuous deformation which evolves an arbitrary non-square quadrilateral into a square, and along the evolution $D(\cdot)$ is strictly increasing. Such continuous deformation rapidly transforms a quadrilateral into a square, eliminating the step of taking the limit of iterations of Steiner symmetrization.

Applying a similar flow vector field, we also prove the following monotonicity result on rectangles, which is also not based on symmetrization, and is new to our knowledge.

Theorem 1.9. *Let R_q be the rectangle with a given area, where $q \geq 1$ is the ratio of the length and the width of the rectangle. Then, $D(R_q)$ is a strictly decreasing function for $q \geq 1$.*

Theorem 1.8 and Theorem 1.9 also have their independent interests, since they serve as monotonicity results on rhombuses and rectangles. The proofs are similar to that of Theorem 1.2.

Outline of the paper In section 2, we derive the evolution equation for $D(\cdot)$ along a smooth flow, and we state some results on boundary properties of $V_\Omega(x) := \int_\Omega K(|x-y|) dy$, which will be crucial in the sign analysis of the derivative of $D(\cdot)$ along flow evolutions. In section 3, we will prove Theorem 1.2 and Theorem 1.3. In section 4, we will prove Theorem 1.5 and Theorem 1.6. In section 5, we will prove Theorem 1.8 and Theorem 1.9. In section 6, we prove Theorem 1.7.

2. BOUNDARY COMPARISON OF V_Ω AND EVOLUTION EQUATION OF $D(\cdot)$ ALONG FLOWS

We first need the following proposition, which is crucial in the sign analysis of the derivative of $D(\cdot)$ along many of the flows utilized in the paper.

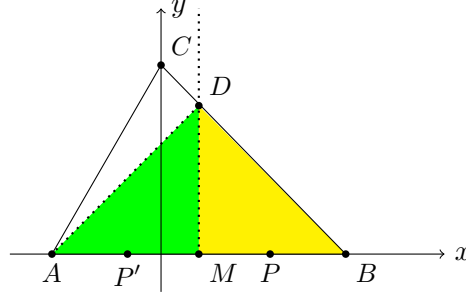
Proposition 2.1. *Let $\Omega = \triangle_{ABC}$ be a triangle with $|BC| > |AC|$. Let M be the midpoint of AB . For any $P \in BM$, let $P' \in AM$ such that $|PM| = |MP'|$. Then, $V_\Omega(P') > V_\Omega(P)$.*

Proof. First, by symmetry, we have

$$\int_{\triangle_{ABD}} K(|PQ|) dQ = \int_{\triangle_{ABD}} K(|P'Q|) dQ.$$

Then, for any $Q \in \text{int}(\triangle_{ACD})$, $|PQ| > |P'Q|$, and hence by the assumption of K , we have

$$\int_{\triangle_{ACD}} K(|PQ|) dQ < \int_{\triangle_{ACD}} K(|P'Q|) dQ.$$

FIGURE 2.1. If $|BC| > |AC|$, then $V_{\Omega}(P) < V_{\Omega}(P')$.

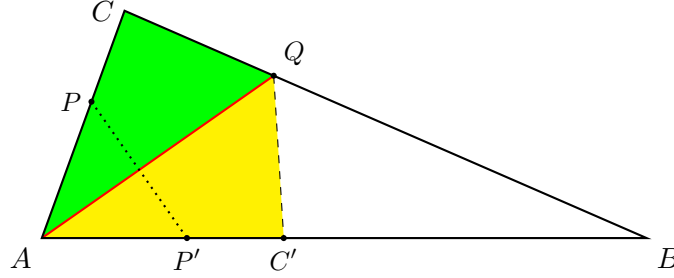
Therefore,

$$\begin{aligned} V_{\Omega}(P) &= \int_{\Delta_{ABD}} K(|PQ|) dQ + \int_{\Delta_{ACD}} K(|PQ|) dQ \\ &< \int_{\Delta_{ABD}} K(|P'Q|) dQ + \int_{\Delta_{ACD}} K(|P'Q|) dQ = V_{\Omega}(P'). \end{aligned}$$

□

Similarly, we have

Proposition 2.2. *Let $\Omega = \Delta_{ABC}$ be a triangle with $|AB| > |AC|$. For any $P \in AC$, $P' \in AB$ with $|PA| = |P'A|$, we have $V_{\Omega}(P') > V_{\Omega}(P)$.*

FIGURE 2.2. If $|AC| < |AB|$, then $V_{\Omega}(P) < V_{\Omega}(P')$.

Proof. Select $Q \in BC$ such that AQ bisects $\angle A$. Let $C' \in AB$ be the reflection point of C about the line segment AQ . For any point $Z \in \Delta_{BC'Q}$, since $|PZ| > |P'Z|$, we have

$$\int_{\Delta_{BC'Q}} K(|PZ|) dZ < \int_{\Delta_{BC'Q}} K(|P'Z|) dZ.$$

Let $D = \Delta_{ACQ} \cup \Delta_{AC'Q}$. Then by symmetry, we have

$$\int_D K(|PZ|) dZ = \int_D K(|P'Z|) dZ.$$

Adding them up, we thus obtain $V_{\Omega}(P) < V_{\Omega}(P')$. □

The next theorem gives the evolution equation for the Riesz-type nonlocal energy $D(\cdot)$ along a flow map generated by a smooth time-dependent vector field. Classical shape derivative formulas are often presented at a particular time, say $t = 0$, see for example [2, Proposition 3.3], while the whole-time evolution equation along a flow is rarely seen in literature and will be of great importance to study the monotonicity properties of $D(\cdot)$ along flow evolutions. Therefore, we also include a proof of the derivation of the evolution equation, which holds in any dimension.

Theorem 2.3. *Let Ω be a piecewise smooth domain in \mathbb{R}^n , $\eta^t(x) := \eta(t, x) : \mathbb{R}_+ \times \mathbb{R}^n \rightarrow \mathbb{R}^n$ be a smooth vector field, and F_t be the flow map generated by η . That is,*

$$\begin{cases} \frac{\partial}{\partial t} F_t(x) = \eta(t, F_t(x)) & t > 0 \\ F_0(x) = x \end{cases}$$

Let $\Omega_t = F_t(\Omega)$. Then for any $t > 0$,

$$\frac{d}{dt} D(\Omega_t) = 2 \int_{\partial\Omega_t} V_{\Omega_t}(x) (\eta^t \cdot \nu) d\sigma,$$

where ν is the outward unit normal to the boundary.

Proof. Let $JF_t = \det(\nabla F_t)$. Then by Jacobi's matrix determinant formula and the chain rule, we have

$$\begin{aligned} \frac{d}{dt} JF_t &= JF_t \operatorname{tr} \left((\nabla F_t)^{-1} \frac{d}{dt} \nabla F_t \right) \\ &= JF_t \operatorname{tr} \left((\nabla F_t)^{-1} \nabla \left(\frac{d}{dt} F_t \right) \right) \\ &= JF_t \operatorname{tr} \left((\nabla F_t)^{-1} \nabla (\eta^t \circ F_t) \right) \\ &= JF_t \operatorname{tr} \left((\nabla F_t)^{-1} (\nabla \eta^t \circ F_t) \nabla F_t \right) \\ &= (\operatorname{div} \eta^t \circ F_t) JF_t. \end{aligned}$$

By the area formula,

$$D(\Omega_t) = \int_{\Omega} \int_{\Omega} K(|F_t(x) - F_t(y)|) JF_t(x) JF_t(y) dx dy.$$

Hence, up to a regularization of the kernel K , (see for example the argument of the proof of [2, Proposition 3.3]), we can take the time derivative inside the integral, and the following

calculation is valid.

$$\begin{aligned}
\frac{d}{dt}D(\Omega_t) &= \int_{\Omega} \int_{\Omega} K'(|F_t(x) - F_t(y)|) \frac{F_t(x) - F_t(y)}{|F_t(x) - F_t(y)|} \cdot (\eta^t(F_t(x)) - \eta^t(F_t(y))) JF_t(x) JF_t(y) dx dy \\
&\quad + 2 \int_{\Omega} \int_{\Omega} K(|F_t(x) - F_t(y)|) \operatorname{div} \eta^t(F_t(x)) JF_t(x) JF_t(y) dx dy \\
&= \int_{\Omega_t} \int_{\Omega_t} K'(|x - y|) \frac{x - y}{|x - y|} (\eta^t(x) - \eta^t(y)) dx dy + 2 \int_{\Omega_t} \int_{\Omega_t} K(|x - y|) \operatorname{div} \eta^t dx dy \\
&= 2 \int_{\Omega_t} \int_{\partial \Omega_t} K(|x - y|) \eta^t(x) \cdot \nu(x) d\sigma_x dy, \\
&\quad \text{by applying the divergence theorem on the second term} \\
&= 2 \int_{\partial \Omega_t} V_{\Omega_t}(x) (\eta^t \cdot \nu) d\sigma, \quad \text{by Fubini's Theorem.}
\end{aligned}$$

□

If we choose F_t to be a translation flow, then we immediately obtain from Theorem 2.3 and the translating invariance of $D(\cdot)$ that, for a triangle $\Omega = \triangle_{ABC}$,

$$\frac{1}{|AB|} \int_{AB} V_{\Omega} ds = \frac{1}{|BC|} \int_{BC} V_{\Omega} ds = \frac{1}{|AC|} \int_{AC} V_{\Omega} ds.$$

This equality is also derived in [2] through the parallel movement of a side, inspired by [4]. This, combined with Proposition 2.2, reveals an intriguing geometric phenomenon: in an arbitrary triangular domain Ω , the longer the side length, the larger the maximum value of V_{Ω} on that side. However, regardless of the side length, the averaged value of V_{Ω} on each side remains the same. Then, a natural question arises: what about the case of rectangles?

Note that similar to the proof of Proposition 2.2, we know that if $\Omega = \square_{ABCD}$ is a rectangle with the condition $|AB| > |AD|$, then

$$\|V_{\Omega}\|_{L^{\infty}(AB)} > \|V_{\Omega}\|_{L^{\infty}(AD)}.$$

Regarding the averaged value of V_{Ω} on each side of the rectangle, quite different from the triangular case, we have:

Proposition 2.4. *Let $\Omega = \square_{ABCD}$ be a rectangle with $|AB| > |AD|$. Then,*

$$\frac{\int_{AB} V_{\Omega} ds}{|AB|} > \frac{\int_{AD} V_{\Omega} ds}{|AD|}. \quad (2.1)$$

This proposition turns out to be crucial to prove Theorem 1.9.

Proof of Proposition 2.4. Without loss of generality, we assume that $A = (0, 0)$, $B = (a, 0)$, $C = (a, b)$ and $D = (0, b)$, with $a > b$. Let E be the point of the intersection of the line $l: y = x$ and the side CD . Let M be the midpoint of AD , N be the midpoint of AB and $M' \in AN$ with $|AM'| = |AM|$. See Figure 2.3 below.

Since the reflection of DE about the line l strictly lies inside the rectangle \square_{ABCD} , for any $P \in AM$, $P' \in AM'$ with $|AP| = |AP'|$, similar to the proof of Proposition 2.2, we have $V_{\Omega}(P) < V_{\Omega}(P')$. By reflection argument and also similar to the proof of Proposition 2.1, we have that V_{Ω} is strictly increasing along the segment AN from A to N . Therefore,

$$\frac{1}{|AM|} \int_{AM} V_{\Omega} ds < \frac{1}{|AM'|} \int_{AM'} V_{\Omega} ds < \frac{1}{|M'N|} \int_{M'N} V_{\Omega} ds.$$

Therefore,

$$\begin{aligned} \frac{1}{|AN|} \int_{AN} V_\Omega ds &= \frac{1}{|AM'| + |M'N|} \left(\int_{AM'} V_\Omega ds + \int_{M'N} V_\Omega ds \right) \\ &> \frac{1}{|AM|} \int_{AM} V_\Omega ds \end{aligned}$$

By symmetry,

$$\frac{1}{|AN|} \int_{AN} V_\Omega ds = \frac{1}{|AB|} \int_{AB} V_\Omega ds, \quad \frac{1}{|AM|} \int_{AM} V_\Omega ds = \frac{1}{|AD|} \int_{AD} V_\Omega ds.$$

Hence (2.1) is obtained. \square

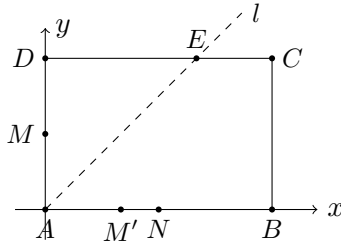


FIGURE 2.3. Picture illustration of the proof of Proposition 2.4

Remark 2.5. *The boundary behavior of V_Ω closely resembles that of the squared norm of the gradient of the torsion function, as evidenced by [8] and [9]. The location of the maximum norm of the gradient of the torsion function is an important problem and has been under extensive research, see [9] and references therein. In particular, [9] demonstrates that for a triangular domain, the maximum of the norm of the gradient of the torsion function uniquely occurs on the longest side, between the midpoint and the foot of the altitude. Furthermore, for nearly equilateral triangles, it is shown that the point of maximum norm is closer to the midpoint. It would be an interesting question itself to derive similar results for V_Ω .*

3. MONOTONICITY OF $D(\cdot)$ ON TRIANGLES VIA HEIGHT STRETCHING AND COMPRESSING FLOWS

In this section, we will prove Theorem 1.2 and Theorem 1.3.

Proof of Theorem 1.2. Without loss of generality, we assume $C = (0, 1)$. Let

$$F_t(x, y) = \frac{1}{\sqrt{1+t}} (x, (1+t)y).$$

Then $F_t(\Omega) = \Omega_t = \triangle_{A_t B_t \tilde{C}_t}$. We construct the following height-stretching time-dependent vector field

$$\eta(t, x, y) = \frac{1}{2} \frac{1}{1+t} (-x, y).$$

Since

$$\frac{\partial}{\partial t} F_t(x, y) = \frac{1}{2} (1+t)^{-3/2} (-x, (1+t)y),$$

we have

$$\frac{\partial}{\partial t} F_t(x, y) = \eta(t, F_t(x, y)).$$

That is, η is exactly the smooth vector field generating the flow map F_t . Hence by Theorem 2.3, we have

$$\frac{d}{dt} D(\Omega_t) = \int_{\partial\Omega_t} \frac{1}{1+t} V_{\Omega_t}((x, y))(-x, y) \cdot \nu \, ds. \quad (3.1)$$

Let $\beta_t = \angle A_t B_t \tilde{C}_t$ and $\gamma_t = \angle B_t A_t \tilde{C}_t$. On $A_t B_t$,

$$(-x, y) \cdot \nu = (-x, y) \cdot (0, -1) = -y = 0.$$

On $B_t \tilde{C}_t$,

$$(-x, y) \cdot \nu = (-x, y) \cdot (\sin \beta_t, \cos \beta_t) = \cos \beta_t (y - x \tan \beta_t).$$

On $A_t \tilde{C}_t$,

$$(-x, y) \cdot \nu = (-x, y) \cdot (-\sin \gamma_t, \cos \gamma_t) = \cos \gamma_t (y + x \tan \gamma_t).$$

Since $\partial\Omega_t = A_t B_t \cup B_t \tilde{C}_t \cup A_t \tilde{C}_t$, by (3.1) and the above, we have

$$\begin{aligned} & \frac{d}{dt} D(\Omega_t) \\ &= \frac{\cos \beta_t}{1+t} \int_{B_t \tilde{C}_t} V_{\Omega_t}((x, y))(y - x \tan \beta_t) \, ds + \frac{\cos \gamma_t}{1+t} \int_{A_t \tilde{C}_t} V_{\Omega_t}((x, y))(y + x \tan \gamma_t) \, ds. \end{aligned}$$

Let M_t be the midpoint of $B_t \tilde{C}_t$. Since $y = (\tan \beta_t)x$ is exactly the line passing through the origin and M_t , for any point $p_t = (x, y) \in B_t M_t$ and $p'_t = (x', y') \in M_t \tilde{C}_t$ with $|p_t M_t| = |p'_t M_t|$, we have

$$0 > y - x \tan \beta_t = -(y' - x' \tan \beta_t).$$

Also, for $-1 < t < t_1$, $|A_t B_t| > |A_t \tilde{C}_t|$, and thus by Proposition 2.1, we have $V_{\Omega_t}(p_t) < V_{\Omega_t}(p'_t)$. Hence

$$\int_{B_t \tilde{C}_t} V_{\Omega_t}((x, y))(y - x \tan \beta_t) \, ds = \int_{B_t M_t} (V_{\Omega_t}(p_t) - V_{\Omega_t}(p'_t)) (y - x \tan \beta_t) \, ds > 0.$$

Similarly, let N_t be the midpoint of side $A_t \tilde{C}_t$. Since $y = -(\tan \gamma_t)x$ is the line passing through the origin and N_t , for any point $q_t = (x, y) \in A_t N_t$ and $q'_t = (x', y') \in N_t \tilde{C}_t$ with $|q_t N_t| = |q'_t N_t|$, we have

$$0 > y + x \tan \gamma_t = -(y' + x' \tan \gamma_t).$$

Again by Proposition 2.1, for any $-1 < t < t_1$, we have

$$\int_{A_t \tilde{C}_t} V_{\Omega_t}((x, y))(y + x \tan \gamma_t) \, ds = \int_{A_t N_t} (V_{\Omega_t}(q_t) - V_{\Omega_t}(q'_t)) (y + x \tan \gamma_t) \, ds > 0.$$

Hence $\frac{d}{dt} D(\Omega_t) > 0$ for any $t \in (-1, t_1)$. This finishes the proof. \square

The proof above is illustrated in Figure 3.1 below.

Next, we prove Theorem 1.3.

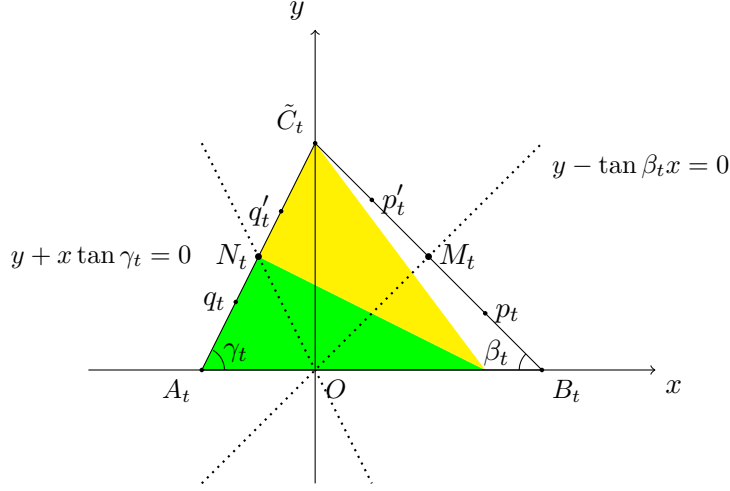


FIGURE 3.1. For $-1 < t < t_1$, $|A_t B_t| > |B_t \tilde{C}_t| \geq |A_t \tilde{C}_t|$. $y = x \tan \beta_t$ and $y = -x \tan \gamma_t$ pass through the midpoints of $B_t \tilde{C}_t$ and $A_t \tilde{C}_t$, respectively. $|p_t M_t| = |p'_t M_t|$, $V_{\Omega_t}(p_t) < V_{\Omega_t}(p'_t)$, $|q_t N_t| = |q'_t N_t|$, $V_{\Omega_t}(q_t) < V_{\Omega_t}(q'_t)$.

Proof of Theorem 1.3. Without loss of generality, we assume that $|OC| = 1$. Let

$$F_t(x, y) = \frac{1}{\sqrt{1-t}}(x, (1-t)y), \quad \eta(t, x, y) = \frac{1}{2(1-t)}(x, -y).$$

Then $\Omega_t = F_t(\Omega)$, and one can check that F_t is generated by the vector field η .

By the similar derivation as in the proof of Theorem 1.2, we have

$$\begin{aligned} \frac{d}{dt} T(\Omega_t) &= \frac{\cos \beta_t}{1-t} \int_{B_t \tilde{C}_t} V_{\Omega_t}((x, y))(x \tan \beta_t - y) ds \\ &\quad + \frac{\cos \gamma_t}{1-t} \int_{A_t \tilde{C}_t} V_{\Omega_t}((x, y))(-x \tan \gamma_t - y) ds, \end{aligned}$$

where $\beta_t = \angle \tilde{C}_t B_t A_t$ and $\gamma_t = \angle \tilde{C}_t A_t B_t$. The similar argument in the proof of Theorem 1.2 also ensures that $\frac{d}{dt} D(\Omega_t) > 0$, for any $t \in (-\infty, t_2)$. \square

To the end, we remark that in Theorem 1.2, if $|AB| > |BC| = |AC|$, then the strict increasing property of $D(\cdot)$ during the shortest height stretching process implies that when $\alpha \in (\pi/3, \pi)$, $D(I(\alpha))$ is a strictly decreasing function. Similarly, if in Theorem 1.3, $|AB| < |BC| = |AC|$, then it implies that when $\alpha \in (0, \pi/3)$, $D(I(\alpha))$ is a strictly increasing function. Therefore, we immediately have our Corollary 1.4.

4. MONOTONICITY OF $D(\cdot)$ ON TRIANGLES VIA LEG STRETCHING AND PARALLEL MOVEMENT FLOW

The main goal of this section is to prove Theorem 1.5 and Theorem 1.6.

To prove Theorem 1.5, it suffices to prove the following theorem:

Theorem 4.1. *Let Ω be a triangle \triangle_{ABC} , where A lies at the origin, B lies on the positive x -axis and $|AB| = |AC|$. Let $B_t = (1+t)B$ and $\Omega_t = \sqrt{|AB|/|AB_t|} \triangle_{AB_t C} = \triangle_{A \tilde{B}_t C_t}$. Then, for $t \in [0, +\infty)$, $D(\Omega_t)$ is a strictly decreasing function.*

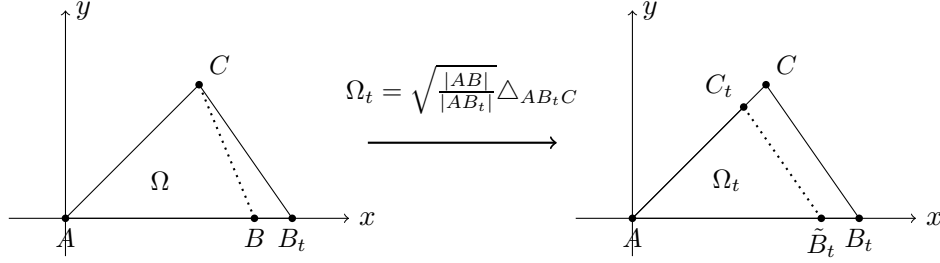


FIGURE 4.1. An illustration of Theorem 4.1. Fix one angle, stretching one leg while scaling to maintain the area as fixed, then $D(\cdot)$ is strictly decreasing.

Proof of Theorem 4.1. Let $\alpha = \angle A$ and $\beta_t = \angle AB_t C = \angle A\tilde{B}_t C_t$. Without loss of generality, we assume that $|AB| = |AC| = 1$. Let

$$G_t(x, y) = ((1+t)x - t(\cot \alpha)y, y).$$

Such G_t is constructed to be a linear mapping which maps B to B_t while keeping A and C fixed. Therefore, G_t maps $\Omega = \triangle_{ABC}$ to the triangle $\triangle_{AB_t C}$, and hence

$$F_t(x, y) := \frac{1}{\sqrt{1+t}} G_t(x, y)$$

maps Ω to Ω_t .

Let

$$\eta(t, x, y) = \frac{1}{2(1+t)} (x - 2(\cot \alpha)y, -y).$$

Such η is obtained by direct computation to guarantee that $\frac{\partial}{\partial t} F_t(x, y) = \eta(t, F_t(x, y))$.

Recall that by Theorem 2.3, we have

$$\frac{d}{dt} D(\Omega_t) = \int_{\partial\Omega_t} 2V_{\Omega_t}((x, y)) \eta(t, x, y) \cdot \nu \, ds.$$

Note that on AC_t , $\nu = (-\sin \alpha, \cos \alpha)$, and thus

$$\eta \cdot \nu = \frac{1}{2(1+t)} (-x \sin \alpha + (\cos \alpha)y) = 0.$$

On $A\tilde{B}_t$, $\nu = (0, -1)$, and thus

$$\eta \cdot \nu = y = 0.$$

On $\tilde{B}_t C_t$,

$$\begin{aligned} \eta \cdot \nu &= \frac{1}{2(1+t)} \left(x - 2 \frac{\cos \alpha}{\sin \alpha} y, -y \right) \cdot (\sin \beta_t, \cos \beta_t) \\ &= \frac{\sin \beta_t}{2(1+t)} \left(x - \left(2 \frac{\cos \alpha}{\sin \alpha} + \frac{\cos \beta_t}{\sin \beta_t} \right) y \right). \end{aligned}$$

Let M_t be the midpoint of $B_t C$ and $\theta_t = \angle M_t A B_t \in (0, \pi/2)$. By the law of sine,

$$|AB_t| = \frac{\sin(\alpha + \beta_t)}{\sin \beta_t}, \quad |B_t M_t| = \frac{1}{2} |B_t C| = \frac{\sin \alpha}{2 \sin \beta_t}.$$

Again by the law of sine,

$$\frac{\sin(\theta_t + \beta_t)}{|AB_t|} = \frac{\sin \theta_t}{|B_t M_t|} \Rightarrow \cot \theta_t = 2 \frac{\cos \alpha}{\sin \alpha} + \frac{\cos \beta_t}{\sin \beta_t}.$$

Hence, on $\tilde{B}_t C_t$,

$$\eta \cdot \nu = \frac{\sin \beta_t}{2(1+t)} (x - (\cot \theta_t) y).$$

Therefore,

$$\frac{d}{dt} D(\Omega_t) = \frac{\sin \beta_t}{\tan \theta_t} \frac{1}{1+t} \int_{\tilde{B}_t C_t} V_{\Omega_t}((x, y)) ((\tan \theta_t) x - y) ds.$$

Now let \tilde{M}_t be the intersection point of the line segment AM_t and the line segment $\tilde{B}_t C_t$, and thus \tilde{M}_t is exactly the midpoint of $\tilde{B}_t C_t$.

Note that for any $p_t = (x, y) \in \tilde{B}_t \tilde{M}_t$, we let $p'_t = (x', y') \in \tilde{M}_t C_t$ such that $|p'_t \tilde{M}_t| = |p_t \tilde{M}_t|$. When $t > 0$, $|A\tilde{B}_t| > |AC_t|$, and thus by symmetry and Theorem 2.1, we have

$$0 < x \tan \theta_t - y = -(x' \tan \theta_t - y'), \quad V_{\Omega_t}(p_t) < V_{\Omega_t}(p'_t).$$

Therefore, for $t > 0$, we have

$$\frac{d}{dt} D(\Omega_t) = \frac{\sin \beta_t}{\tan \theta_t} \frac{1}{(1+t)} \int_{\tilde{B}_t \tilde{M}_t} (V_{\Omega_t}(p_t) - V_{\Omega_t}(p'_t)) (x \tan \theta_t - y) ds < 0.$$

This finishes the proof. \square

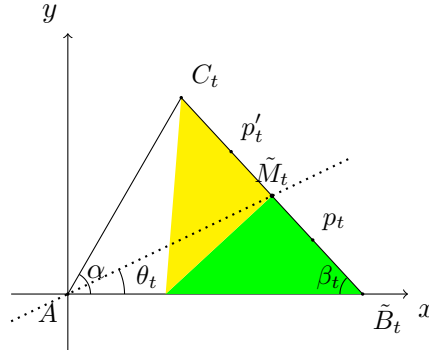


FIGURE 4.2. An illustration of the proof of Theorem 4.1. $\Omega_t = \triangle_{A\tilde{B}_t C_t}$. For any $t > 0$, $|AB_t| > |AC_t|$. \tilde{M}_t is the midpoint of $\tilde{B}_t C_t$, $\theta_t = \angle \tilde{B}_t A \tilde{M}_t$. If $|p_t \tilde{M}_t| = |p'_t \tilde{M}_t|$, then $V_{\Omega_t}(p_t) < V_{\Omega_t}(p'_t)$.

Next, we will prove Theorem 1.6, and it suffices to prove the following theorem.

Theorem 4.2. *Let $\Omega = \triangle_{ABC}$ be the quadrilateral with vertices $A = (-b, h)$, $B = (a, 0)$, $C = (-a, 0)$, where $a, b, h > 0$. Let $A_t = ((t-1)b, h)$ and $\Omega_t = \triangle_{A_t BC}$. Then, $D(\Omega_t)$ is strictly increasing when $-\infty < t \leq 1$.*

The argument in the proof of Theorem 4.1 no longer works. Instead, slightly adapting the argument in [2] can conclude Theorem 4.2. The original idea is from [3].

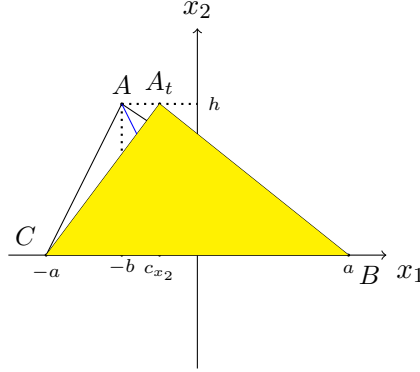


FIGURE 4.3. Parallel movement of top vertex

Proof of Theorem 4.2. Let

$$\Phi_t(x_1, x_2) := \left(x_1 + \frac{x_2}{h}bt, x_2 \right).$$

Then Φ_t is a smooth mapping that transforms Ω into Ω_t , and Ω_1 becomes an isosceles triangle with $|A_1C| = |A_1B|$.

For any $x_2 \in \mathbb{R}$, we let

$$P_{x_2} = \{x_1 \in \mathbb{R} : (x_1, x_2) \in \Omega\}.$$

Hence

$$P_{x_2} = (c_{x_2} - r_{x_2}, c_{x_2} + r_{x_2}),$$

where $c_{x_2} = -x_2b/h$ and $r_{x_2} = a(h - x_2)/h$.

For any fixed $x_2, y_2 \in (0, h)$, we define $K_l(r) = K(\sqrt{l^2 + r^2})$, where $l = |x_2 - y_2|$. Hence

$$\begin{aligned} D(\Omega_t) &= \int_{\Omega_t} \left(\int_{\Omega_t} K \left(\sqrt{(x_1 - y_1)^2 + (x_2 - y_2)^2} \right) dx_1 dx_2 \right) dy_1 dy_2 \\ &= \int_0^h \int_0^h I_{K_l}[P_{x_2}, P_{y_2}](t) dx_2 dy_2, \end{aligned}$$

where

$$I_{K_l}[P_{x_2}, P_{y_2}](t) = \int_{\Phi_t(P_{y_2})} \int_{\Phi_t(P_{x_2})} K_l(x_1 - y_1) dx_1 dy_1.$$

Since

$$c_{x_2} - c_{y_2} = \frac{b}{h}(y_2 - x_2),$$

we can rewrite

$$\begin{aligned} I_{K_l}[P_{x_2}, P_{y_2}](t) &= \int_{c_{y_2} - r_{y_2} + \frac{b}{h}y_2t}^{c_{y_2} + r_{y_2} + \frac{b}{h}y_2t} \int_{c_{x_2} - r_{x_2} + \frac{b}{h}x_2t}^{c_{x_2} + r_{x_2} + \frac{b}{h}x_2t} K_l(x_1 - y_1) dx_1 dy_2 \\ &= \int_{-r_{y_2}}^{r_{y_2}} \int_{-r_{x_2}}^{r_{x_2}} K_l \left(x_1 - y_1 + c_{x_2} - c_{y_2} + \left(\frac{b}{h}x_2 - \frac{b}{h}y_2 \right) t \right) dx_1 dy_1 \\ &= \int_{-r_{y_2}}^{r_{y_2}} \int_{-r_{x_2}}^{r_{x_2}} K_l \left(x_1 - y_1 + \frac{b}{h}(x_2 - y_2)(t - 1) \right) dx_1 dy_1. \end{aligned}$$

Let

$$M_t := \frac{b}{h}(x_2 - y_2)(t - 1),$$

and hence

$$\begin{aligned} \frac{d}{dt} I_{K_l}[P_{x_2}, P_{y_2}](t) &= \frac{b}{h}(x_2 - y_2) \int_{-r_{y_2}}^{r_{y_2}} \int_{-r_{x_2}}^{r_{x_2}} K_l'(x_1 - y_1 + M_t) dx_1 dy_1 \\ &= \frac{b}{h}(x_2 - y_2) \int_{-r_{y_2}}^{r_{y_2}} \int_{-r_{x_2} + M_t}^{r_{x_2} + M_t} K_l'(x_1 - y_1) dx_1 dy_1. \end{aligned}$$

If $x_2 < y_2$, then for $t < 1$, $M_t > 0$. Let $R_t = (-r_{x_2} + M_t, r_{x_2} + M_t) \times (-r_{y_2}, r_{y_2})$, $E = R_t \cap \{(x_1, y_1) : y_1 > x_1\}$ and E' be the reflection of E about the origin. Let $\Sigma = R_t \setminus (E \cup E')$. Then in this case, Σ is a non-empty rectangle lying inside $\{(x_1, y_1) : x_1 - y_1 > 0\}$, as illustrated in Figure 4.4. Since $K_l'(r)$ is an odd function and $K_l'(r) < 0$ if $r > 0$, we have

$$\frac{d}{dt} I_{K_l}[P_{x_2}, P_{y_2}](t) = \frac{b}{h}(x_2 - y_2) \iint_{\Sigma} K_l'(x_1 - y_1) dx_1 dy_1 > 0.$$

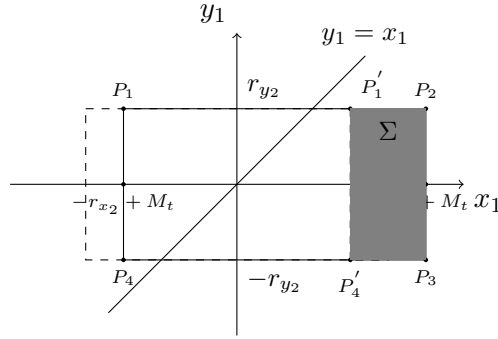


FIGURE 4.4. The case of $x_2 < y_2$ and thus $M_t > 0$.

Similarly, if $x_2 > y_2$, we still have $\frac{d}{dt} I_{K_l}[P_{x_2}, P_{y_2}](t) > 0$, for $t < 1$. Therefore, for any $-\infty < t < 1$, we have

$$\frac{d}{dt} D(\Omega_t) = \int_0^h \int_0^h \frac{d}{dt} I_{K_l}[P_{x_2}, P_{y_2}](t) dx_2 dy_2 > 0.$$

□

5. MONOTONICITY RESULTS OF $D(\cdot)$ ON RHOMBUSES AND RECTANGLES VIA VERTICAL STRETCHING FLOWS

In this section, we prove Theorem 1.8 and Theorem 1.9. The proof is based on the same stretching flow argument as in the proof of Theorem 1.2.

First, to prove Theorem 1.8, it suffices to prove the following, which gives the monotonicity of $D(\cdot)$ along the continuous diagonal-stretching deformation on a rhombus.

Theorem 5.1. *Let R_t , $t \geq 0$ be a family of rhombuses with vertices $A = (-a, 0)$, $B_t = (0, -a(1+t))$, $C = (a, 0)$, $D_t = (0, a(1+t))$, where $a > 0$. Let $\Omega_t = \frac{1}{\sqrt{1+t}} R_t$. Then,*

$$\frac{d}{dt} D(\Omega_t) \leq 0,$$

where the equality holds if and only if $t = 0$.

Proof. Without loss of generality, we assume that $a = 1$. Again, we let

$$F_t(x, y) = \frac{1}{\sqrt{1+t}}(x, (1+t)y), \quad \eta(t, x, y) = \frac{1}{2} \frac{1}{1+t}(-x, y).$$

Then $F_t(R_0) = \Omega_t$ and η is the smooth vector field generating the flow map F_t .

Let $A_t = \frac{1}{\sqrt{1+t}}A$, $\tilde{B}_t = \frac{1}{\sqrt{1+t}}B_t$, $C_t = \frac{1}{\sqrt{1+t}}C$, and $\tilde{D}_t = \frac{1}{\sqrt{1+t}}D_t$. By Theorem 2.3 and the symmetry, we have

$$\frac{d}{dt}D(\Omega_t) = \frac{4}{1+t} \int_{C_t \tilde{D}_t} V_{\Omega_t}((x, y))(-x, y) \cdot \nu \, ds,$$

Note that on $C_t \tilde{D}_t$,

$$(-x, y) \cdot \nu = (-x, y) \cdot (\sin \theta_t, \cos \theta_t) = \cos \theta_t(y - (\tan \theta_t)x),$$

where $\theta_t = \angle ACD_t$.

Hence

$$\frac{d}{dt}D(\Omega_t) = \frac{4 \cos \theta_t}{1+t} \int_{C_t \tilde{D}_t} V_{\Omega_t}((x, y)) (y - (\tan \theta_t)x) \, ds.$$

Let M_t be the midpoint of $C_t \tilde{D}_t$. For any $p_t = (x, y) \in C_t M_t$ and $p'_t = (x', y') \in M_t \tilde{D}_t$ with $|p_t M_t| = |p'_t M_t|$, we have by the geometry of the rhombus and the reflection method (similar to the proof of Theorem 2.1) that

$$V_{\Omega_t}(p_t) \geq V_{\Omega_t}(p'_t),$$

with " $>$ " holding if and only if $t = 0$.

Also, $-(y' - x' \tan \theta_t) = y - x \tan \theta_t < 0$. Hence

$$\frac{d}{dt}D(\Omega_t) = \frac{4 \cos \theta_t}{1+t} \int_{C_t M_t} (V_{\Omega_t}(p_t) - V_{\Omega_t}(p'_t)) (y - x \tan \theta_t) \, ds \leq 0,$$

where the equality holds if and only if $t = 0$. This finishes the proof. \square

Next, we prove Theorem 1.9. Clearly, to prove it, it suffices to prove the following theorem.

Theorem 5.2. *Let $R = \square ABCD$ be the square with vertices $A = (0, 0)$, $B = (b, 0)$, $C = (b, b)$ and $D = (0, b)$, $b > 0$. Let $C_t = (b, (1+t)b)$, $D_t = (0, (1+t)b)$ and $R(t) = \square ABC_t D_t$ be the rectangle with vertices A, B, C_t, D_t . Let $\Omega_t = \frac{1}{\sqrt{1+t}}R(t)$. Then, for any $t \geq 0$,*

$$\frac{d}{dt}D(\Omega_t) \leq 0,$$

where the equality holds if and only if $t = 0$.

Proof. Without loss of generality, we assume $b = 1$. As before, we let

$$F_t(x, y) = \frac{1}{\sqrt{1+t}}(x, (1+t)y), \quad \eta(t, x, y) = \frac{1}{2} \frac{1}{1+t}(-x, y).$$

Then $F_t(R) = \Omega_t$ and η is the smooth vector field generating the flow map F_t .

Let $B_t = \frac{1}{\sqrt{1+t}}B$, $\tilde{C}_t = \frac{1}{\sqrt{1+t}}C_t$, and $\tilde{D}_t = \frac{1}{\sqrt{1+t}}D_t$. Then $\Omega = \square AB_t \tilde{C}_t \tilde{D}_t$ is the rectangle with vertices $A, B_t, \tilde{C}_t, \tilde{D}_t$. Clearly, $|B_t \tilde{C}_t| = \frac{1}{\sqrt{1+t}}|BC| = \sqrt{1+t}$, and $|\tilde{C}_t \tilde{D}_t| = \frac{1}{\sqrt{1+t}}$.

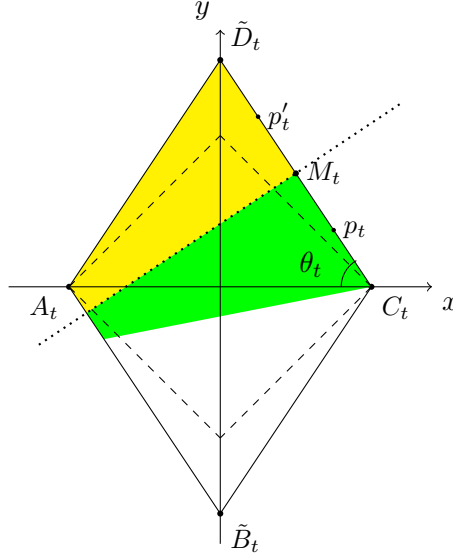


FIGURE 5.1. An illustration of the proof of Theorem 5.1. The reflection of the yellow part is strictly inside the rhombus Ω_t .

Since $\eta \cdot \nu = 0$ on $AB_t \cup A\tilde{D}_t$, by Theorem 2.3, we have

$$\begin{aligned} \frac{d}{dt}D(\Omega_t) &= \frac{1}{1+t} \int_{B_t\tilde{C}_t} V_{\Omega_t}((x, y))(-x, y) \cdot (1, 0) ds + \frac{1}{1+t} \int_{\tilde{C}_t\tilde{D}_t} V_{\Omega_t}((x, y))(-x, y) \cdot (0, 1) ds \\ &= \frac{1}{1+t} \left(-\frac{1}{\sqrt{1+t}} \int_{B_t\tilde{C}_t} V_{\Omega_t}((x, y)) ds + \sqrt{1+t} \int_{\tilde{C}_t\tilde{D}_t} V_{\Omega_t}((x, y)) ds \right) \\ &= \frac{1}{1+t} \left(\frac{1}{|\tilde{C}_t\tilde{D}_t|} \int_{\tilde{C}_t\tilde{D}_t} V_{\Omega_t}((x, y)) ds - \frac{1}{|B_t\tilde{C}_t|} \int_{B_t\tilde{C}_t} V_{\Omega_t}((x, y)) ds \right) \end{aligned}$$

When $t = 0$, $|\tilde{C}_t\tilde{D}_t| = |B_t\tilde{C}_t| = 1$, and hence $\frac{d}{dt}D(\Omega_t) = 0$. When $t > 0$, $|\tilde{C}_t\tilde{D}_t| < |B_t\tilde{C}_t|$, and hence by Proposition 2.4 and above, $\frac{d}{dt}D(\Omega_t) < 0$. This finishes the proof. \square

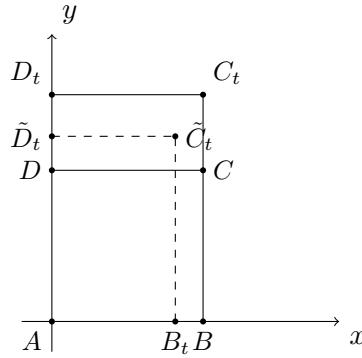


FIGURE 5.2. An illustration of Theorem 5.2. $|\square AB_t\tilde{C}_t\tilde{D}_t| = |\square ABCD|$

6. CONTINUOUS MONOTONIC DEFORMATION OF QUADRILATERALS

In this section, we first prove Theorem 1.7. The proof will be divided into two cases.

Case 1: A_0 and C_0 lie on the same side of the x_2 -axis. That is, $x_A x_C > 0$, where x_A and x_C are the first coordinates of A_0 and C_0 , respectively. Then it suffices to prove the following:

Proposition 6.1. *Let $\Omega = \square_{ABCD}$ be the square with vertices $A = (-b_1, h_1)$, $B = (a, 0)$, $C = (-b_2, -h_2)$, $D = (-a, 0)$, where $a, b_1, b_2, h_1, h_2 > 0$. Let $A_t = (-b_1(1-t), h_1)$ and $C_t = (-b_2(1-t), -h_2)$, $\Omega_t = \square_{A_t B C_t D}$. Then, $D(\Omega_t)$ is strictly increasing when $-\infty < t \leq 1$.*

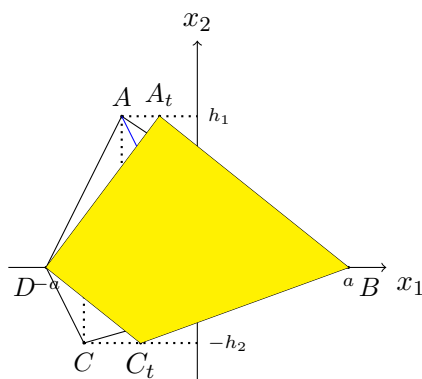


FIGURE 6.1. A and C lie in the same side of the x_2 -axis

Proof. Let

$$\Phi_t(x_1, x_2) := \begin{cases} \left(x_1 + \frac{b_1}{h_1} x_2 t, x_2 \right), & x_2 \geq 0 \\ \left(x_1 - \frac{b_2}{h_2} x_2 t, x_2 \right), & x_2 < 0 \end{cases}$$

Then Φ_t is a smooth mapping that transforms Ω into Ω_t . As in the proof of Theorem 4.2, we let

$$P_{x_2} = \{x_1 \in \mathbb{R} : (x_1, x_2) \in \Omega\} = (c_{x_2} - r_{x_2}, c_{x_2} + r_{x_2}),$$

where in this case,

$$c_{x_2} = \begin{cases} -\frac{x_2}{h_1} b_1, & x_2 \geq 0 \\ \frac{x_2}{h_2} b_2, & x_2 < 0 \end{cases}$$

and

$$r_{x_2} = \begin{cases} \frac{a}{h_1} (h_1 - x_2), & x_2 \geq 0 \\ \frac{a}{h_2} (h_2 + x_2), & x_2 < 0 \end{cases}$$

For any fixed $x_2, y_2 \in (0, h)$, we define $K_l(r) = K(\sqrt{l^2 + r^2})$, where $l = |x_2 - y_2|$. Hence

$$\begin{aligned} \frac{d}{dt}D(\Omega_t) &= \int_0^{h_1} \int_0^{h_1} \frac{d}{dt}I_{K_l}[P_{x_2}, P_{y_2}](t) dx_2 dy_2 + 2 \int_{-h_2}^0 \int_0^{h_1} \frac{d}{dt}I_{K_l}[P_{x_2}, P_{y_2}](t) dx_2 dy_2 \\ &\quad + \int_{-h_2}^0 \int_{-h_2}^0 \frac{d}{dt}I_{K_l}[P_{x_2}, P_{y_2}](t) dx_2 dy_2 \\ &=: I + II + III, \end{aligned}$$

where

$$I_{K_l}[P_{x_2}, P_{y_2}](t) = \int_{\Phi_t(P_{y_2})} \int_{\Phi_t(P_{x_2})} K_l(x_1 - y_1) dx_1 dy_1.$$

As in the proof of Theorem 4.2, for $t < 1$, we have $I > 0$ and $III > 0$.

For $x_2 \in [0, h_1]$, $y_2 \in [-h_2, 0)$, we have

$$\begin{aligned} I_{K_l}[P_{x_2}, P_{y_2}](t) &= \int_{c_{y_2} - r_{y_2} - \frac{b_2}{h_2} y_2 t}^{c_{y_2} + r_{y_2} - \frac{b_2}{h_2} y_2 t} \int_{c_{x_2} - r_{x_2} + \frac{b_1}{h_1} x_2 t}^{c_{x_2} + r_{x_2} + \frac{b_1}{h_1} x_2 t} K_l(x_1 - y_1) dx_1 dy_1 \\ &= \int_{-r_{y_2}}^{r_{y_2}} \int_{-r_{x_2}}^{r_{x_2}} K_l\left(x_1 - y_1 + c_{x_2} - c_{y_2} + \frac{b_1}{h_1} x_2 t + \frac{b_2}{h_2} y_2 t\right) dx_1 dy_1 \end{aligned}$$

Let

$$M_t := c_{x_2} - c_{y_2} + \frac{b_1}{h_1} x_2 t + \frac{b_2}{h_2} y_2 t = \left(\frac{b_1}{h_1} x_2 + \frac{b_2}{h_2} y_2 \right) (t - 1)$$

Then

$$\frac{d}{dt}I_{K_l}[P_{x_2}, P_{y_2}](t) = \left(\frac{b_1}{h_1} x_2 + \frac{b_2}{h_2} y_2 \right) \int_{-r_{y_2}}^{r_{y_2}} \int_{-r_{x_2} + M_t}^{r_{x_2} + M_t} K'_l(x_1 - y_1) dx_1 dy_1.$$

Since for $t < 1$, $\frac{b_1}{h_1} x_2 + \frac{b_2}{h_2} y_2$ and M_t have opposite signs, similar to the proof of Theorem 4.2, we also have $II > 0$ for $t < 1$.

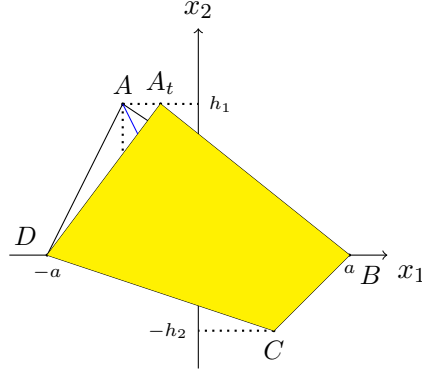
Therefore, we conclude the proposition. \square

Case 2: A_0 and C_0 lie on two different sides of the x_2 -axis. That is, $x_A x_C \leq 0$. Then it suffices to prove the following stronger result.

Proposition 6.2. *Let $\Omega = \square_{ABCD}$ be the quadrilateral with vertices $A = (-b_1, h_1)$, $B = (a, 0)$, $C = (b_2, -h_2)$, $D = (-a, 0)$, where $a, b_1, h_1, h_2 > 0$, and $b_2 \geq 0$. Let $A_t = (b_1(t - 1), h_1)$ and $\Omega_t = \square_{A_t B C D}$. Then, $D(\Omega_t)$ is strictly increasing when $-\infty < t \leq 1$.*

Proof. Let

$$\Phi_t(x_1, x_2) := \begin{cases} \left(x_1 + \frac{x_2}{h_1} b_1 t, x_2 \right), & x_2 \geq 0 \\ (x_1, x_2), & x_2 < 0 \end{cases},$$

FIGURE 6.2. A and C lie on two different sides of the x_2 -axis

and thus $\Omega_t = \Phi_t(\Omega)$. Again,

$$\begin{aligned} \frac{d}{dt}D(\Omega_t) &= \int_0^{h_1} \int_0^{h_1} \frac{d}{dt} I_{K_l} [P_{x_2}, P_{y_2}](t) dx_2 dy_2 + 2 \int_{-h_2}^0 \int_0^{h_1} \frac{d}{dt} I_{K_l} [P_{x_2}, P_{y_2}](t) dx_2 dy_2 \\ &\quad + \int_{-h_2}^0 \int_{-h_2}^0 \frac{d}{dt} I_{k_l} [P_{x_2}, P_{y_2}](t) dx_2 dy_2 \\ &=: I + II + III, \end{aligned}$$

where

$$c_{x_2} = \begin{cases} -\frac{x_2}{h_1} b_1, & x_2 \geq 0 \\ -\frac{x_2}{h_2} b_2, & x_2 < 0 \end{cases}$$

$$r_{x_2} = \begin{cases} \frac{a}{h_1} (h_1 - x_2), & x_2 \geq 0 \\ \frac{a}{h_2} (h_2 + x_2), & x_2 < 0 \end{cases}$$

and

$$P_{x_2} := \{x_1 \in \mathbb{R}, (x_1, x_2) \in \Omega\} = (c_{x_2} - r_{x_2}, c_{x_2} + r_{x_2}).$$

Similar to the proof of Theorem 4.2, $I > 0$. Also, it is clear that $III = 0$.

If $0 < x_2 < h_1$ and $-h_2 < y_2 < 0$, then

$$\begin{aligned} I_{K_l} [P_{x_2}, P_{y_2}](t) &= \int_{c_{y_2} - r_{y_2}}^{c_{y_2} + r_{y_2}} \int_{c_{x_2} - r_{x_2} + \frac{b_1}{h_1} x_2 t}^{c_{x_2} + r_{x_2} + \frac{b_1}{h_1} x_2 t} K_l(x_1 - y_1) dx_1 dy_1 \\ &= \int_{-r_{y_2}}^{r_{y_2}} \int_{-r_{x_2}}^{r_{x_2}} K_l \left(x_1 - y_1 + c_{x_2} + \frac{b_1}{h_1} x_2 t - c_{y_2} \right) dx_1 dy_1 \\ &= \int_{-r_{y_2}}^{r_{y_2}} \int_{-r_{x_2}}^{r_{x_2}} K_l(x_1 - y_1 + M_t) dx_1 dy_1, \end{aligned}$$

where

$$M_t = -\frac{x_2}{h_1} b_1 + \frac{y_2}{h_2} b_2 + \frac{b_1}{h_1} x_2 t = \frac{b_1}{h_1} x_2 (t - 1) + \frac{y_2}{h_2} b_2. \quad (6.1)$$

Hence

$$II = 2 \int_{-h_2}^0 \int_0^{h_1} \frac{b_1 x_2}{h_1} \left(\int_{-r_{y_2}}^{r_{y_2}} \int_{-r_{x_2} + M_t}^{r_{x_2} + M_t} K'_t(x_1 - y_1) dx_1 dy_1 \right) dx_2 dy_2.$$

From (6.1), when $t < 1$, $x_2 > 0$ and $y_2 < 0$, we have $M_t < 0$. Then, the similar argument in the proof of Theorem 4.2 implies that $II > 0$.

Therefore, we conclude that $D(\Omega_t)$ is a strictly increasing function for $-\infty < t \leq 1$. □

Combining Proposition 6.1 and Proposition 6.2, we obtain Theorem 1.7.

We note that any quadrilateral must be of either type I (the case in Proposition 6.1) or type II (the case in Proposition 6.2). The following pictures Figure 6.3 and Figure 6.4 illustrate a continuous deformation of an arbitrary quadrilateral into a square, along which $D(\cdot)$ is strictly increasing, as a consequence of Theorem 1.8, Proposition 6.1 and Proposition 6.2. This gives another proof of the fact that the square maximizes $D(\cdot)$ among quadrilaterals with a given area, without resorting to the limit process of step-by-step Steiner symmetrizations as used in [2].

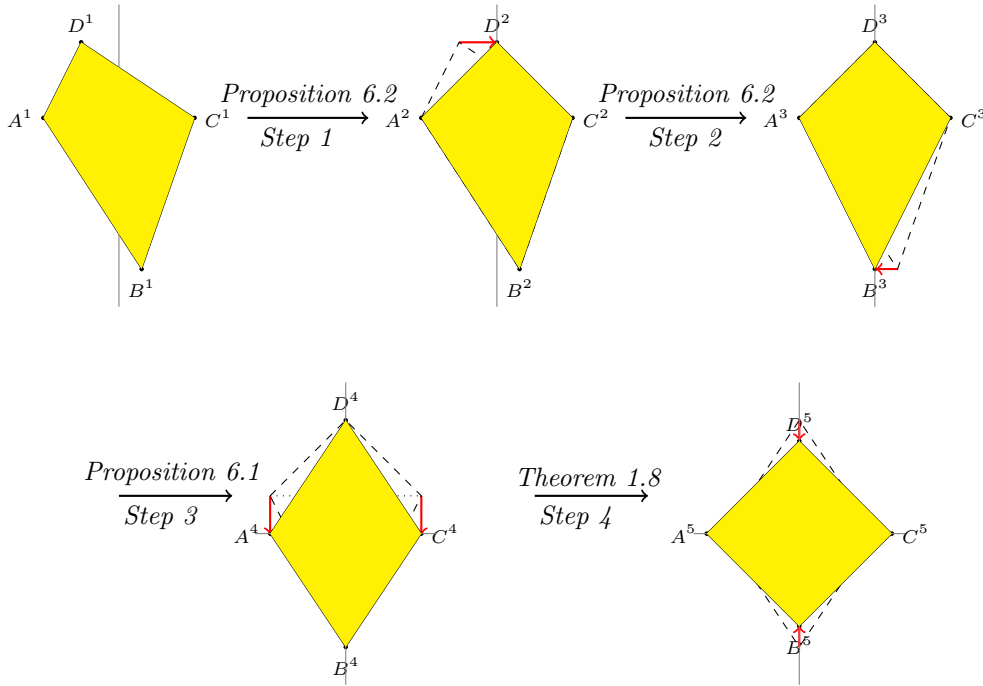


FIGURE 6.3. Type I: continuous monotonic deformation for $D(\cdot)$

Remark 6.3. *In fact, as can be observed from Proposition 6.2, the first and second steps in Figure 6.3 can be carried out simultaneously. This establishes the monotonicity of property $D(\cdot)$ under the classical continuous Steiner symmetrization with respect to the direction perpendicular to the diagonal, thereby proving Theorem 1.7.*

Remark 6.4. *Proposition 6.2 indeed gives a stronger result: within the Type I case, we can further decompose the continuous Steiner symmetrization process as a two-step partial*

continuous symmetrization: continuously symmetrizing one portion and leaving the other one fixed. The partial continuous symmetrization still guarantees the strict monotonicity property of $D(\cdot)$, as illustrated in Figure 6.3.

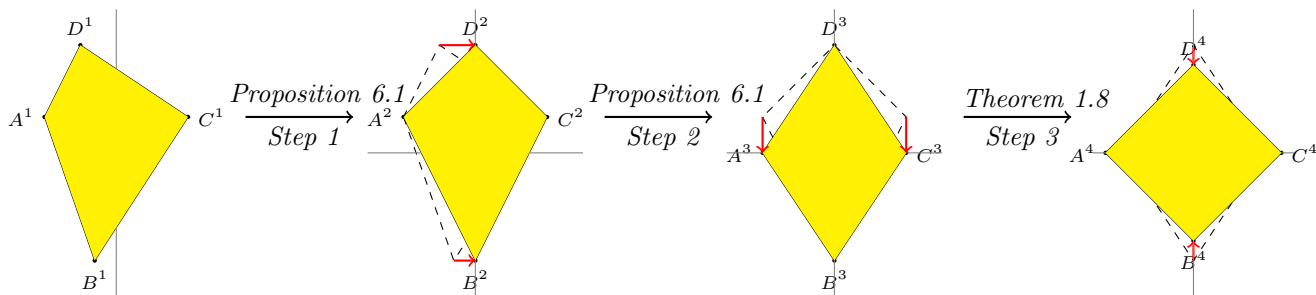


FIGURE 6.4. Type II: continuous monotonic deformation for $D(\cdot)$

Data Availability Statement: This study is a theoretical analysis, and no new data were created or analyzed. Therefore, data sharing is not applicable to this article.

REFERENCES

- [1] Bogosel B, Bucur D, Fragalà I. The nonlocal isoperimetric problem for polygons: Hardy–Littlewood and Riesz inequalities. *Mathematische Annalen*. 2024 Jun;389(2):1835-82.
- [2] Bonacini M, Cristoferi R, Topaloglu I. Riesz-type inequalities and overdetermined problems for triangles and quadrilaterals. *The Journal of Geometric Analysis*. 2022 Feb;32(2):48.
- [3] Carrillo JA, Hittmeir S, Volzone B, Yao Y. Nonlinear aggregation-diffusion equations: radial symmetry and long time asymptotics. *Inventiones mathematicae*. 2019 Dec;218:889-977.
- [4] Fragalà I, Velichkov B. Serrin-type theorems for triangles. *Proceedings of the American Mathematical Society*. 2019 Apr;147(4):1615-26.
- [5] J. Hadamard, Mémoire sur le problème d’analyse relatif l’équilibre des plaques élastiques encastées. *Mémoires des Savants Etrangers*, 33 (1908).
- [6] Henrot A. *Extremum problems for eigenvalues of elliptic operators*. Springer Science & Business Media, 2006.
- [7] Henrot A. *Shape optimization and spectral theory*, De Gruyter Open, Warsaw, 2017.
- [8] Huang Y, Li Q, Xie S, Yang H. Flow approach on the monotonicity of shape functionals. arXiv preprint. arXiv 2502.09485.
- [9] Li Q, Xie S, Yang H, et al. On location of maximal gradient of torsion function over some non-symmetric planar domains. arXiv preprint arXiv:2406.04790, 2024.
- [10] Pólya G, Szegő G. *Isoperimetric Inequalities in Mathematical Physics*.(AM-27) 2016.
- [11] Siudeja B. Isoperimetric inequalities for eigenvalues of triangles. *Indiana University mathematics journal*. 2010 Jan 1:1097-120.
- [12] Riesz F. Sur une inégalité intégrale. *J. Lond. Math. Soc.* 5(3), 162–168 (1930)
- [13] Solynin A Y. Exercises on the theme of continuous symmetrization. *Computational Methods and Function Theory*, 2020, 20: 465-509.

SCHOOL OF MATHEMATICS, HUNAN UNIVERSITY, CHANGSHA, HUNAN, CHINA.

Email address: 17773612125@163.com

SCHOOL OF MATHEMATICS, HUNAN UNIVERSITY, CHANGSHA, P.R. CHINA.

Email address: liqinfeng1989@gmail.com

DEPARTMENT OF MATHEMATICS, THE CHINESE UNIVERSITY OF HONG KONG, HONG KONG.

Email address: wei@math.cuhk.edu.hk

SCHOOL OF MATHEMATICS, HUNAN UNIVERSITY, CHANGSHA, P.R. CHINA.

Email address: hangyang0925@gmail.com